Phenomenological study of quarkonium suppression and the impact of the energy gap between singlets and octets

Jean-Paul Blaizot
Institut de Physique Théorique, Université Paris Saclay, CEA, CNRS, F-91191 Gif-sur-Yvette, France

Miguel Ángel Escobedo
Instituto Galego de Física de Altas Enerxías (IGFAE), Universidade de Santiago de Compostela, E-15782 Galicia, Spain

(Received 8 July 2021; accepted 27 August 2021; published 27 September 2021)

The study of heavy quarkonium suppression in heavy-ion collisions represents an important source of information about the properties of the quark-gluon plasma produced in such collisions. In a previous paper, we have considered how to model the evolution of a quarkonium in such a way that the solution of the resulting equations evolves toward the correct thermal equilibrium distribution for a homogeneous and static medium. We found that it is crucial to take into account the energy gap between singlet and octet configurations when the temperature is not much greater than this energy gap. In this paper, we explore in more detail the phenomenological consequences of this observation in the more realistic situation of an expanding system. We consider two different scenarios, based on the same approximation scheme, but on different choices of parameters. In the first case, we rely on a Hard Thermal Loop approximation, while the second case is based on a recent determination of the static potential in lattice QCD. In both cases, we compute the decay width and the nuclear modification factor, both taking the energy gap into account and ignoring it. We find that the impact on the predictions is as large in the expanding medium as it is in the static case. Our conclusion is that this energy gap should be taken into account in phenomenological studies.

DOI: 10.1103/PhysRevD.104.054034

I. INTRODUCTION

Several physical phenomena are commonly invoked to explain the production of quarkonia in ultra-relativistic heavy-ion collisions that are presently intensively studied at the LHC [1–3]. Aside from the initial suggestion of the color screening of the binding potential by the quark-gluon plasma [4], collisions between the plasma constituents and the quarkonia could also lead to a suppression of the production rate. Various methods can be used to take these collisions into account. In the regime in which potential models are valid, it has been shown that collisions induce an imaginary part in the potential [5,6] (somewhat analogous to the imaginary potential of the nuclear optical potential model). In the effective theory picture where the interactions of quarkonia with the plasma are dominated by color dipolar interactions, collisions induce singlet to octet transitions [7]. In addition to these "suppression" mechanisms, there is also the possibility, when the number of heavy quarks created in a heavy-ion collision is large enough, that uncorrelated heavy quarks recombine to form a bound state inside the medium. This process, usually called recombination [8,9], appears to be an important contribution to charmonium production at present collider energies.

The construction of a robust formalism that takes into account consistently all three mechanisms is a challenging task. In recent years, it has been found useful to consider the various approaches from the perspective of open quantum systems, the "system" being the quarkonia, interacting with the quark-gluon plasma considered as "environment" [10–22]. Recent reviews can be found in [23,24]. This formalism allows us to compute the evolution of bound states in a medium, taking into account quantum mechanical effects. In this way, it has been understood that quantum coherence [25] is essential at high temperatures when the binding energy is of the order of the decay width. At the same time, semiclassical equations can be derived rigorously from the open quantum system framework in special limits [13,18,20–22]. This has improved the understanding of the validity region of these semiclassical approaches. The common assumption in most, if not all,

approaches is that the medium is moderately affected by the presence of quarkonia. Various types of effective theories can then be obtained for the heavy quark dynamics, with further approximations becoming available, depending on the energy or time scales.

In the limit in which the temperature, T, is much bigger than the binding energy, E, the interaction between a quarkonium and the medium is Markovian. In this case, the dynamics is governed by a Gorini–Kossakowski–Sudarshan–Lindblad (GKSL) equation [26,27]. Phenomenological predictions of quarkonium in heavy-ion collisions using the GKSL equation in the $T \gg E$ limit have been discussed in [14,15,28]. However, as was understood in [21], this limit leads to a maximization of the entropy without taking into account energy conservation constraints. In other words, this approximation does not lead to the correct thermalization. In [21], we showed that, when $T \sim E$, the decay width is modified to include a dependence on the binding energy. With a slight abuse of language, we can say that the imaginary part of the potential depends on the energy. This dependence is a key element which guarantees that the evolution equation complies with the fluctuation-dissipation theorem. Phenomenologically, it is important to take this dependence into account when the temperature is not much larger than the binding energy, as was shown numerically in [29].

The aim of this paper is to emphasize the importance of the energy dependence of the decay width, not only in the case of a static medium, but also in a more realistic case of an expanding medium. We do this by computing the nuclear modification factor, R_{AA}, in different scenarios. For each scenario, we compare the results obtained with and without the energy dependence of the imaginary part of the potential. We observe that, depending on the centrality of the collision, the productions of $\Upsilon(1S)$ and $\Upsilon(2S)$ are significantly less suppressed when we take into account the energy dependence. We emphasize that our purpose here is just to obtain an estimate of the effect, and show that it is indeed quite significant. We shall not go into a detailed analysis of experimental data.

The manuscript is organized as follows. In Sec. II, we review the model that we developed in [21] and we discuss the imaginary part of the potential and its energy dependence. In Sec. III, we use this model to obtain phenomenological predictions of R_{AA} using two different scenarios, one based on (resummed) perturbation theory, and another scenario in which we use lattice QCD inputs. Finally, we present our conclusions in Sec. IV.

II. DISCUSSION OF THE MODEL

The model that we consider in the present paper is an extension of that introduced in the last section of [21]. Let us recall briefly its origin. One starts from the evolution equation for the reduced density matrix $\mathcal{D}_Q$ of a pair of heavy quarks in a quark-gluon plasma, the interaction of the heavy quarks with the plasma, supposed to be weak, being limited to a one-gluon exchange. The plasma is assumed to be in thermal equilibrium at a temperature T. This equation reads [21]

$$\begin{aligned}&\frac{\mathrm{d}\mathcal{D}_Q}{\mathrm{d}t}+i[H_Q,\mathcal{D}_Q(t)]\\&=-g^2\int_{\boldsymbol{x}\boldsymbol{x}'}\int_0^{t-t_0}\mathrm{d}\tau[n^A_{\boldsymbol{x}},U_Q(\tau)n^A_{\boldsymbol{x}'}U_Q^\dagger(\tau)\mathcal{D}_Q(t)]\Delta^>(\tau;\boldsymbol{x}-\boldsymbol{x}'))\\&\quad-g^2\int_{\boldsymbol{x}\boldsymbol{x}'}\int_0^{t-t_0}\mathrm{d}\tau[\mathcal{D}_Q(t)U_Q(\tau)n^A_{\boldsymbol{x}'}U_Q^\dagger(\tau),n^A_{\boldsymbol{x}}]\Delta^<(\tau;\boldsymbol{x}-\boldsymbol{x}').\end{aligned}\tag{1}$$

Here, H_Q is the Hamiltonian that governs the dynamics of the heavy quark pair in vacuum, with the corresponding evolution operator given by $U_Q(t)=\mathrm{e}^{-iH_Qt}$. $n^A_{\boldsymbol{x}}$ is the temporal component of the color current, whose explicit expression can be found in [20]. The interaction between the heavy quarks and the surrounding medium is captured by the correlators of thermal fluctuations of the gluon fields a^A_0,

$$\begin{aligned}&\mathrm{Tr}_{\mathrm{pl}}[a^A_0(t,\mathbf{x})a^B_0(t',\mathbf{y})\mathcal{D}_{\mathrm{pl}}]=\delta^{AB}\Delta^>(t-t',\mathbf{x}-\mathbf{y}),\\&\mathrm{Tr}_{\mathrm{pl}}[a^B_0(t',\mathbf{y})a^A_0(t,\mathbf{x})\mathcal{D}_{\mathrm{pl}}]=\delta^{AB}\Delta^<(t-t',\mathbf{x}-\mathbf{y}),\end{aligned}\tag{2}$$

where $\mathcal{D}_{\mathrm{pl}}$ is the density matrix of the plasma, and A, B are color indices of the adjoint representation. We ignore here the color magnetic interactions, which are subleading for heavy quarks.

As was shown in detail in [21] this general equation can be simplified through a number of steps:

(i) A part of the right-hand side of Eq. (1), which is hermitian, can be absorbed in a redefinition of H_Q. This can be done by adding to both sides of Eq. (1)

$$\begin{aligned}&\frac{g^2}{2}\int_{\boldsymbol{x}\boldsymbol{x}'}\int_0^{t-t_0}\mathrm{d}\tau[n^A_{\boldsymbol{x}}n^A_{\boldsymbol{x}'},\mathcal{D}_Q(t)](\Delta^>(\tau;\boldsymbol{x}-\boldsymbol{x}')\\&\quad-\Delta^<(\tau;\boldsymbol{x}-\boldsymbol{x}')).\end{aligned}\tag{3}$$

In the left-hand side, this is considered to be a correction to the real part of the potential, while in the right-hand side, it remains a compensating correction. From now on, H_Q denotes the heavy quark hamiltonian after this redefinition.

(ii) By projecting Eq. (1) on the eigenstates of H_Q, with $H_Q|i\rangle=E_i|i\rangle$, one gets

$$\frac{d\mathcal{D}_{ij}}{dt}+iE_{ij}\mathcal{D}_{ij}=\mathcal{L}_{ij,kl}\mathcal{D}_{kl},\tag{4}$$

where $\mathcal{D}_{ij}=\langle i|\mathcal{D}_Q|j\rangle$, $E_{ij}=E_i-E_j$, and $\mathcal{L}_{ij,kl}\mathcal{D}_{kl}$ are a rewriting of the right-hand side of Eq. (1) from which the hermitian contribution to H_Q has been subtracted.

(iii) When the typical time between collisions of the quarkonium with plasma constituents is much bigger than the inverse of the binding energy, which we shall assume to be the case, $\mathcal{L}_{ij,kl}$ can be treated as a perturbation. The multiple-scale analysis described in Appendix B of [21] provides a way to handle the secular terms which appear in the perturbative expansion. Assuming for simplicity that there are no degenerate states, we obtain then an equation for the diagonal part of the density matrix, namely for the probabilities $p_i = D_{ii}$:

$$\frac{dp_i}{dt} = \mathcal{L}_{ii,kk} p_k. \tag{5}$$

(iv) A final simplification arises from the analysis of the color degrees of freedom. We are interested in the probability to find the quarkonium in a singlet state at the end of the evolution. By emitting or absorbing gluons, a color singlet can decay into an octet, and vice versa a singlet can emerge from an octet. We shall restrict ourselves to the dilute limit where there are only a few heavy quarks in the medium. This situation is appropriate for bottomonium production at the LHC. The study of charmonium would concern the dense limit with a large number of heavy quarks present in the medium. This is a much more difficult problem, which has only been addressed so far in special limits [20] (see also [13] for the analogous Abelian case), or using the Boltzmann equation [18,19]. In the case of bottomonium, we have checked numerically that the contribution from octet decays is tiny. The reason is that octets are unbound and may occupy all the volume of the medium, while a bound color singlet occupies a small volume. Therefore, in the dilute limit, the rate of the octet to singlet transitions decreases as the volume of the medium increases. Besides, this transition is also suppressed in the large N_c limit [30]. Finally, we arrive at a simple rate equation,

$$\frac{dp_s}{dt} = -\Gamma_s p_s, \tag{6}$$

for the probability p_s of finding the quarkonium in a singlet state. In the next subsection we analyze the properties of the decay rate Γ_s.

A. Properties of Γ_s

The decay width Γ_s is given by the following formula [21]:

$$\Gamma_s = 8\pi\alpha_s C_F \int_{\mathbf{p}} \mathrm{e}^{-\frac{E^o_{\mathbf{p}} - E^s}{T}} \int_{\mathbf{q}} \Delta^{>}(E^o_{\mathbf{p}} - E^s, \mathbf{q}) \times \left| \langle \mathrm{s}| \sin\left(\frac{\mathbf{q}\cdot\hat{\mathbf{r}}}{2}\right) |\mathrm{o}, \mathbf{p}\rangle \right|^2, \tag{7}$$

where the operator, $\sin(\frac{\mathbf{q}\cdot\hat{\mathbf{r}}}{2})$, with $\hat{\mathbf{r}}$ (an operator acting on the heavy quark relative coordinates) describes the interaction of the quarkonium with the gluons of the plasma, after the center of mass of the quarkonium has been integrated out [21]. In the limit of small momentum transfer q, it reduces to a dipolar interaction, as we shall discuss shortly. In Eq. (7), $|s\rangle$ is the wave function of the singlet and E_s its binding energy. The ket $|\mathrm{o}, \mathbf{p}\rangle$ is the state of a heavy quark pair in an octet state with energy $E^{\mathrm{o}}_{\mathbf{p}} = \frac{p^2}{M}$. In the large N_c limit the octet potential is zero; therefore, the wave function of an octet can be approximated by a plane wave. As a consequence, the expectation value $\langle \mathrm{s}| \sin(\frac{\mathbf{q}\hat{\mathbf{r}}}{2}) |\mathrm{o}, \mathbf{p}\rangle$ is easily obtained as a Fourier transform of the wave function of the singlet bound state. The last ingredient needed to compute the decay width is the correlator $\Delta^{>}(w, \mathbf{q})$ [see Eq. (2)]. We shall estimate it using the Hard Thermal Loop (HTL) approximation [32–34].

$$\Delta^{>}(w, \mathbf{q}) = \frac{\mathrm{e}^{w/T}}{\mathrm{e}^{w/T} - 1} \sigma(w, \mathbf{q}), \tag{8}$$

where

$$\sigma(\omega, \mathbf{q}) = \frac{2\mathrm{Im}\Pi_L(\omega, \mathbf{q})}{(q^2 + \mathrm{Re}\Pi_L(\omega, \mathbf{q}))^2 + (\mathrm{Im}\Pi_L(\omega, \mathbf{q}))^2} \tag{9}$$

and

$$\Pi_L(\omega, \mathbf{q}) = m_D^2(T) \left(1 - \frac{\omega}{2q} \ln\left(\frac{\omega + q + i\epsilon}{\omega - q + i\epsilon}\right)\right) \tag{10}$$

is the longitudinal component of the gluon polarization tensor. It is proportional to the Debye mass m_D, given in leading order perturbation theory by

$$m_D(T) = \sqrt{\frac{4\pi\alpha_s(N_c + T_F N_F)}{3}} T, \tag{11}$$

where $N_c = 3$, $T_F = \frac{1}{2}$, and N_F is the number of flavors that can be considered light when computing m_D (we take $N_F = 3$). A plot of this Debye mass as a function of the temperature, as obtained with different scales for the running coupling constant α_s, is given in Fig. 1. One can see that (for this range of temperatures) $m_D \simeq 2.5T$, a result that is not truly in the perturbative regime. Thus we should regard our use of the HTL result as a convenient phenomenological guide, providing us with a reasonable approximation for the overall momentum and frequency dependence of the longitudinal tensor, while m_D, to which it is proportional, could be viewed as a phenomenological parameter.

If one ignores the gap between singlets and octets, which may be legitimate when the temperature is high enough, one obtains the simpler expression

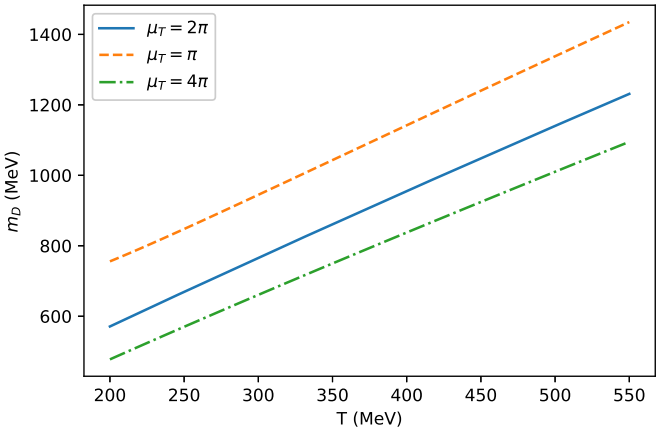

FIG. 1. Perturbative Debye mass as a function of the temperature, estimated from Eq. (11) with the running coupling constant α_s evaluated at different values of the scale μ_T.

$$\Gamma_s^0 = 8\pi\alpha_s C_F \int_{\mathbf{q}} \Delta^>(0,\mathbf{q})\langle \mathrm{s}|\sin^2\left(\frac{\mathbf{q}\hat{\mathbf{r}}}{2}\right)|\mathrm{s}\rangle, \qquad (12)$$

which we refer to as the static limit [35]. This expression (12) can be read as twice the imaginary part of the potential, as originally computed in [5]. One may then interpret Eq. (7) in similar terms, as an energy dependent imaginary potential. This energy dependence, present in the exponential factor as well as in the correlator, plays a crucial role at low temperature since it ensures that the fluctuation-dissipation theorem is fulfilled. The impact of this energy dependence of the imaginary potential was studied numerically in [21], and is illustrated in Fig. 2. One can see that ignoring this energy dependence typically increases the decay width by a factor of 2. The purpose of this note is to quantify this effect in the more realistic situation of an expanding plasma. We note that the importance of the energy gap was recognized in early studies of quarkonium interactions with matter [36,37].

Before closing this subsection, we note that the energy dependence in Eq. (7) originates from the energy gap between singlets and octets. We determine the singlet binding energy by solving the Schrödinger equation

$$H_Q|\mathrm{s}\rangle = E_s|\mathrm{s}\rangle, \qquad H_Q = \frac{p^2}{M} + V_s(r). \qquad (13)$$

The potential V_s is a screened potential which will be specified shortly. At this point we will just comment on the interplay between screening and decay rate:

(i) For simplicity, we set the origin of energies as that of the lowest energy octet state. Then the absolute value of the gap between a singlet state and the octet is equal to the binding energy of the singlet. Then, for the model to be valid, the condition $|E_s| \gg \Gamma_s$ must be fulfilled. This is equivalent to saying that the time scale for which thermal effects become important must be much larger than the inverse of typical energy difference between states. If this is not so, we cannot consider thermal effects as a perturbation using multiple-scale analysis [see the discussion before Eq. (5)], which is crucial to get to the simple form of Eq. (6).

(ii) The decay width increases rapidly as the gap decreases. Therefore, the phenomena of screening and decay due to the collisions influence each other. As the temperature increases, so does screening. Screening reduces the energy gap between singlets and octets, and this results in an increase of the decay width.

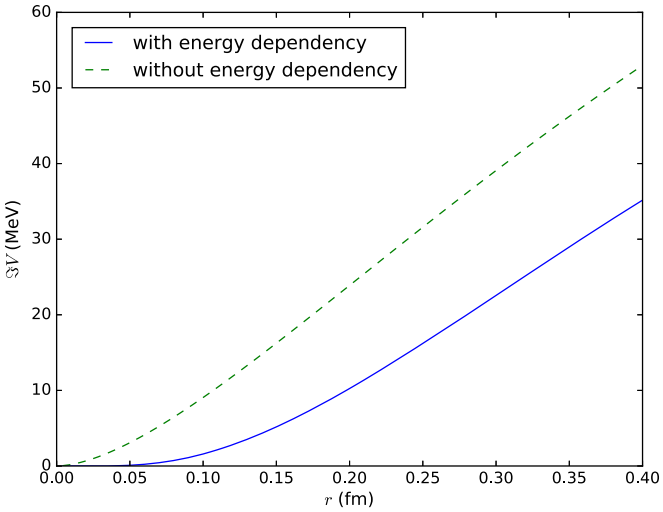

FIG. 2. Comparison between the imaginary part of the potential at $T = 250$ MeV obtained from Eq. (7) (with energy dependency) or from Eq. (12) (without energy dependency). Note that the effect of energy dependence is sizeable and amounts to typically a factor 2 reduction. Picture taken from [21].

Because of this strong interplay, it is important to have a consistent and simultaneous treatment of both phenomena.

B. Relation with the dipole approach

At this point we wish to make a comment on the dipole approximation used in most effective field theory calculations based on the assumption of a clean separation of scales. In the (strict) limit $\frac{1}{r} \gg m_D \gg \Delta E$, Eq. (12) reduces to

$$\Gamma_s^0 \sim 2\pi\alpha_s(\mu_T) C_F \int_{\mathbf{q}} q^i q^j \Delta^>(0,\mathbf{q})\langle s|r^i r^j|s\rangle. \qquad (14)$$

This expression is plagued by an ultraviolet divergence whose origin can be found in the HTL approximation used for the gluon propagator. This approximation is only valid for $q \lesssim m_D$, which is in principle compatible with our assumption. However, in expanding the sine function, assuming that $qr \ll 1$, we have produced a factor $q^i q^j$ whose magnitude is not controlled anymore by any factor.

The HTL correlator results then integrated over momenta where it is not valid. This is the origin of the divergence. This divergence can be coped with by introducing a cutoff Λ in the q-integration, using the HTL approximation of the correlator for $q < \Lambda$ and the full one-loop correlator for $q > \Lambda$. Since the divergence is logarithmic, the dependence on the cutoff eventually disappears, leaving contributions proportional to $\ln(T/m_D)$. We should note however that such a logarithm, while positive in the strict perturbative regime where $T \gg m_D$, may turn negative in the temperature range probed by present experiments (where the coupling constant may remain of order unity), leading to unphysical values for the decay rate.

An alternative to the procedure outlined above is to use a better approximation for the correlator $\Delta^{>}(0,\mathbf{q})$ in Eq. (14). We can rewrite this equation as [14,15]

$$\Gamma_s^0 \sim \frac{\pi\alpha_s(\mu_T)}{3N_c}\int dt\langle\nabla^i A_0^A(t,\mathbf{0})\nabla^i A_0^A(0,\mathbf{0})\rangle\langle s|r^2|s\rangle \sim \langle s|r^2|s\rangle\kappa, \tag{15}$$

with κ being a momentum diffusion coefficient [38]. This formula relates this diffusion coefficient to the correlator of electric field fluctuations, and this can be calculated beyond the HTL approximation, including possibly nonperturbative effects [39]. A detailed discussion of these issues can be found in [23]. Here we note that in the important regime where the various scales are overlapping, a static diffusion constant is in any case not enough, since it ignores the frequency dependence which we claim is important.

We now present details of the implementations of the model and examine two scenarios to fix the parameters. For lack of better terminology, we shall refer to these scenarios as the perturbative scenario and the lattice scenario. It should be understood however that the perturbative scenario departs from strict perturbation theory (as we have already alluded to) and the lattice scenario is not a lattice calculation.

C. The perturbative scenario

We obtain the binding energy and the wave functions needed to compute Γ_s and Γ_s^0 by solving numerically the Schrödinger equation, using the algorithm described in [40]. We focus on $\Upsilon(1S)$ because it is only for this state that, within this scenario, the condition that the binding energy is much bigger than the decay width is fulfilled. This condition is needed for Eq. (6) to be valid. In the case of $\Upsilon(2S)$, the decay width is of the same magnitude as the binding energy at the lowest temperature that we consider. We need to specify first the hamiltonian H_Q in Eq. (13). For M, we take as definition a naive version of the 1S of mass [41], which consists in setting $M = \frac{M_{\Upsilon(1S)}}{2} \sim 4730$ MeV. We think that, given the accuracy we are aiming at, this is a reasonable option.

For the real part of the potential, we use a screened Yukawa potential,

$$V_s(r) = -\frac{C_F\alpha_s(\mu_r)e^{-m_D(T,\mu_T)r}}{r}, \tag{16}$$

where μ_r and μ_T are (independent) subtraction points. The scale μ_r is related to the exchange of gluons between the heavy quark and the antiquark and enters the running coupling α_s in Eqs. (7) and (16). A natural choice would be $\mu_r \sim \frac{1}{r}$, but this would lead to difficulties at large distance r in the numerical implementation of the running coupling. Therefore we fix $\mu_r \sim \frac{1}{a_0}$, where a_0 is the Bohr radius, which we define with the following self-consistent equation:

$$\frac{1}{a_0} = \frac{MC_F\alpha_s(1/a_0)}{2}, \qquad a_0 = 0.149 \text{ fm}. \tag{17}$$

The scale μ_T is the scale at which α_s is evaluated when computing the Debye mass using Eq. (11). The Debye mass encodes the influence of the particles with a typical energy of order πT, which is therefore a natural choice for the value of μ_T. Finally, we use the leading order β-function for the running of the coupling constant, with $\Lambda_{\rm QCD} = 250$ MeV and $N_F = 3$.

Figure 3 illustrates various criteria that are often considered for the melting of the quarkonia. The one based on screening states that the bound state disappears when $\langle r\rangle$, the average size of the bound state, becomes comparable to the Debye screening length $\sim 1/m_D$. Thus one expects screening alone to affect the survival of bound states when $\langle rm_D\rangle$ becomes of order unity. The other criterion focuses on collisions and considers that the bound state disappears when the decay width Γ_s becomes of comparable magnitude as the binding energy E_s, that is when Γ_s/E_s becomes

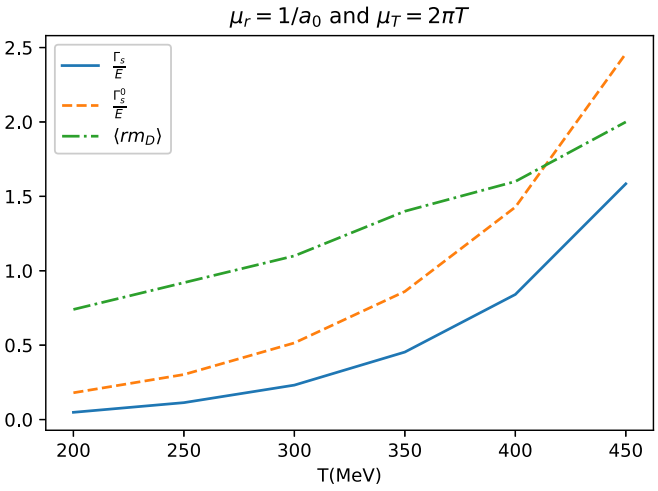

FIG. 3. Comparison of the dimensionless quantities $\langle rm_D\rangle$, $\frac{\Gamma_s}{E}$, and $\frac{\Gamma_s^0}{E}$. The subtraction points are $\mu_r = \frac{1}{a_0}$ and $\mu_T = 2\pi T$.

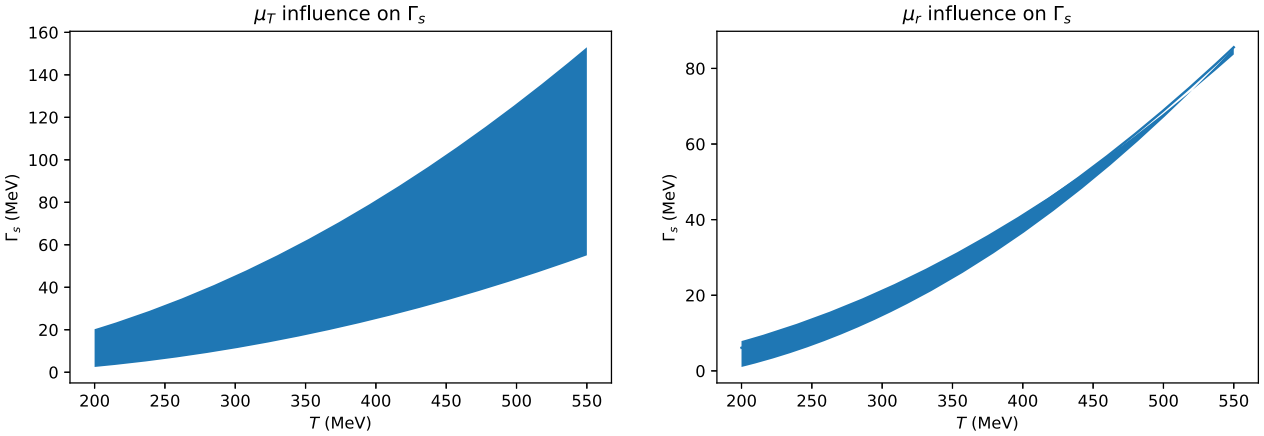

FIG. 4. These plots illustrate the influence of μ_T (left) and μ_r (right) on Γ_s. In the left plot, $\mu_r = \frac{1}{a_0}$ while $\mu_T = \pi T, 2\pi T, 4\pi T$. In the right plot $\mu_T = 2\pi T$, and $\mu_r = \frac{1}{2a_0}, \frac{1}{a_0}, \frac{2}{a_0}$.

of order unity. We note that both $\langle rm_D \rangle$ and Γ_s/E_s are increasing functions of the temperature. Figure 3 also illustrates the influence of the gap by comparing the ratios Γ_s/E and Γ_s^0/E_s. We remind that the model is valid as long as this ratio is well below 1.

Consider now the uncertainty that results from the choices of μ_r and μ_T in the computation of the decay width. We only computed Γ_s and Γ_s^0 for a finite set of temperatures (increasing T from 200 to 450 MeV by steps of 50 MeV) to save on computational cost. However, we have observed that the following function provides a good fit of our results:

$$\Gamma_s \sim aT + bT^2. \tag{18}$$

There is no theoretical reason for choosing this fit function apart from the fact that at very high energies one expects the decay to grow linearly with the temperature (neglecting the running of the coupling). This fit function will be used later when we calculate the R_{AA} for the expanding system. Here this is used as an interpolation formula to estimate the error associated with the choices of the various subtraction scales. Figures 4 and 5 illustrate the sensitivity of, respectively, Γ_s and Γ_s^0 to variations of μ_r and μ_T around nominal values, chosen to be $1/a_0$ and $2\pi T$, respectively. Clearly the uncertainty associated with variations of μ_T is bigger than that associated to changes in μ_r. Overall, we observe that $\Gamma_s^0 > \Gamma_s$, as expected.

D. The lattice scenario

As an alternative possibility for fixing the basic ingredients of the model, we shall rely on the lattice data from a recent computation [42]. We refer to this second strategy as the "lattice scenario." As in the perturbative scenario, the binding energy and the wave function of the quarkonia are obtained by solving a Schrödinger equation. However, now we take as the heavy quark mass the same as in [42], $M = 4882$ MeV, slightly larger than that of the perturbative scenario. As for the real part of the potential, it is given by

$$V_s(r) = -\frac{\alpha e^{-m_D r}}{r} - \sigma r e^{-m_D r}\left(1 + \frac{2}{m_D r}\right), \tag{19}$$

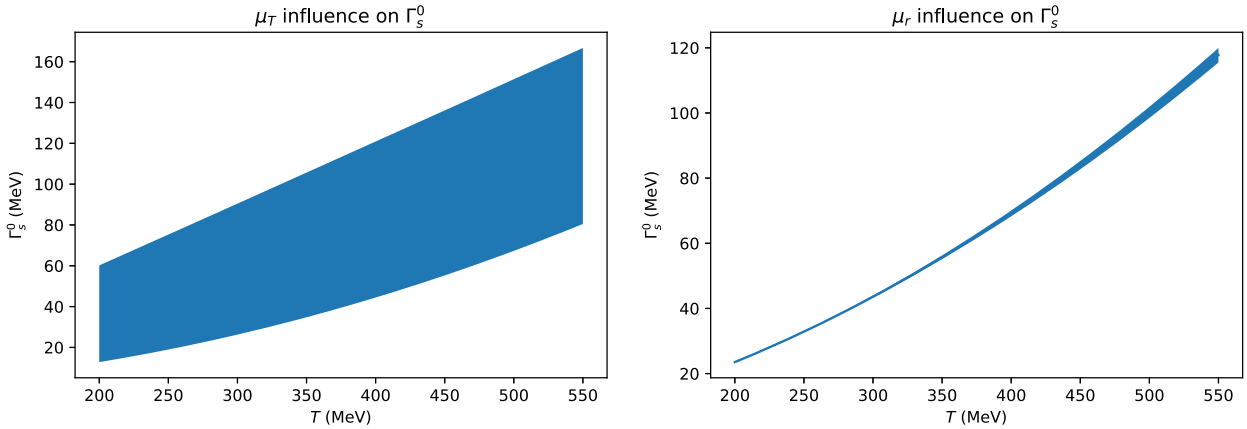

FIG. 5. Same as Fig. 4 but for Γ_s^0.

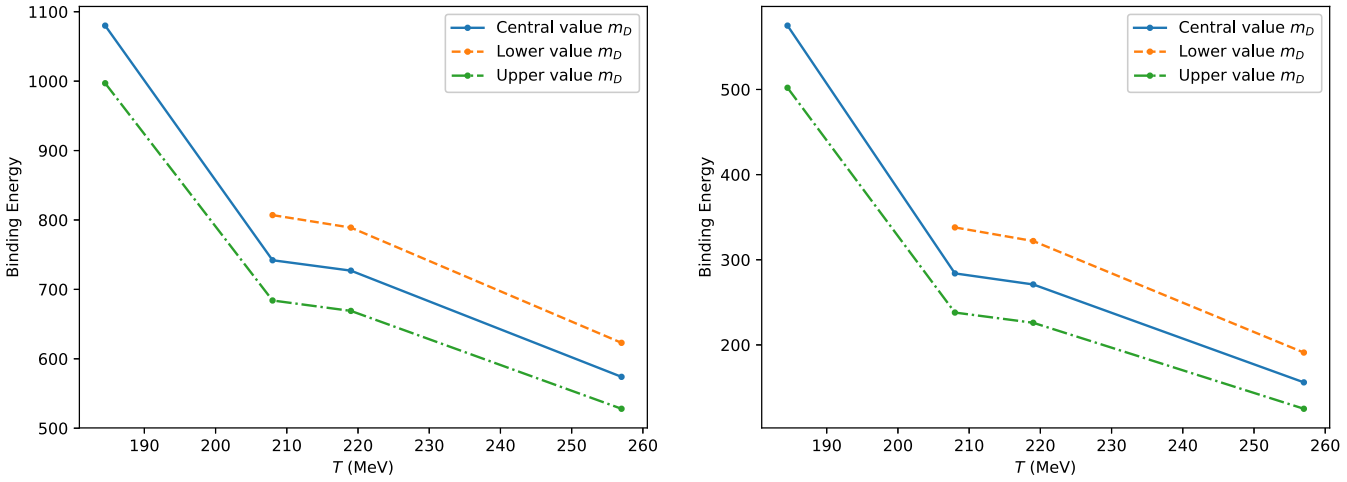

FIG. 6. Binding energy of $\Upsilon(1S)$ (left) and $\Upsilon(2S)$ (right) in the strongly coupled scenario.

where α, σ, and m_D are obtained from the fit performed in [42]. The values of m_D differ from those in the perturbative scenario, and they are given at a different set of temperatures. These values are listed in Table I together with the corresponding temperatures at which they are determined. The definition of the potential is such that $V_s(\infty) = 0$, i.e., states become unbound at $E = 0$. We identify therefore $-E_{1S}$ as the energy gap between the 1S state and the octets, with E_{1S} the binding energy. It may happen that, at low temperature, the solution of the Schrödinger equation with the potential (19) yields a binding energy larger than that obtained at $T = 0$ and computed as $2M_B - M_\Upsilon$, where M_B is the mass of a B meson and M_Υ the mass of the $\Upsilon(1S)$. We discard such cases as unphysical. This is somewhat similar to what is done in Eq. (3.5) of [43]. This is why no result is given in Fig. 6 for $T = 184.5$ MeV and the lowest value of m_D.

The decay width is obtained from Eq. (7), with the values of m_D now listed in Table I, and $\alpha_s = \alpha/C_F$ with α taken from [42]. With these parameters, it becomes possible to study both $\Upsilon(1S)$ and $\Upsilon(2S)$ since for both states the condition $E_s > \Gamma_s$ is fulfilled. The results of the calculation are displayed in Fig. 6 for the binding energy and in Figs. 7 and 8 for the decay widths Γ_s and Γ_s^0, respectively.

In the case of the $\Upsilon(1S)$, the decay width is well fitted by the formula

$$\Gamma_s \sim \tilde{a} T e^{-\frac{\tilde{b}}{T}}, \tag{20}$$

TABLE I. Debye mass as a function of temperature as extracted from the fit in [42].

T (MeV)	m_D (MeV)
184.5	317 ± 25
208	437.5 ± 29.5
219	445 ± 30
257	534 ± 33

motivated in part by the fact that at high temperatures the decay width is linear with the temperature while at small temperatures we expect an exponential suppression due to the gap. For the case of $\Upsilon(2S)$, however, we found that Eq. (18) works better as a fit function. These formulae are used in the analysis presented in Figs. 7 and 8. We note that the fact that we use the same fit function for $\Upsilon(2S)$ as we did for $\Upsilon(1S)$ in the perturbative scenario does not imply that our computation for $\Upsilon(2S)$ is perturbative.

The biggest source of error in this lattice scenario comes from the value of m_D. We consider three cases, referred to as S1, S2, and S3. The case S1 uses the central value of m_D. The cases S2 and S3 correspond respectively to the lowest (S2) or the largest (S3) values of m_D that are compatible with the error given in [42]. The resulting fit parameters are given in Table II. Using these parameters we obtain the decay widths of $\Upsilon(1S)$ and $\Upsilon(2S)$ shown in Fig. 7. Note that these figures contain an extrapolation to temperatures that are larger than those available in the lattice calculations (which are limited to $T \leq 260$ MeV).

The results we have obtained for the binding energy and the decay width can be compared to recent results in the literature. The binding energies that we have obtained for $\Upsilon(1S)$ and $\Upsilon(2S)$ are shown in Fig. 6. For $\Upsilon(1S)$ these are qualitatively similar and of the same order of magnitude as those in [44–48]. For $\Upsilon(2S)$, our results are qualitatively similar to those in [44,45] but about five times smaller than those found in [47], in which the decay width is not based in the HTL model but rather on the computation in [49]. Concerning the decay width, we note that, in general, we obtain results for the $\Upsilon(1S)$ that are of the same order of magnitude as those in [44–48], however, the qualitative behavior is different since our results are more suppressed at small temperatures. The reason is that we take into account the suppression due to the energy gap between singlet and octet states, which was not taken into account in the other studies. We observe a similar behavior in the case

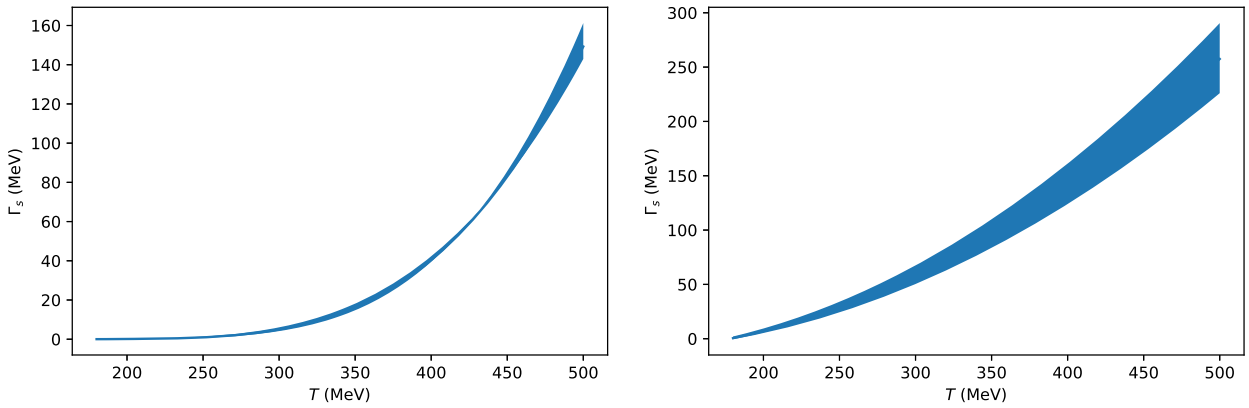

FIG. 7. The decay width Γ_s of $\Upsilon(1S)$ (left) and $\Upsilon(2S)$ (right) in the lattice scenario.

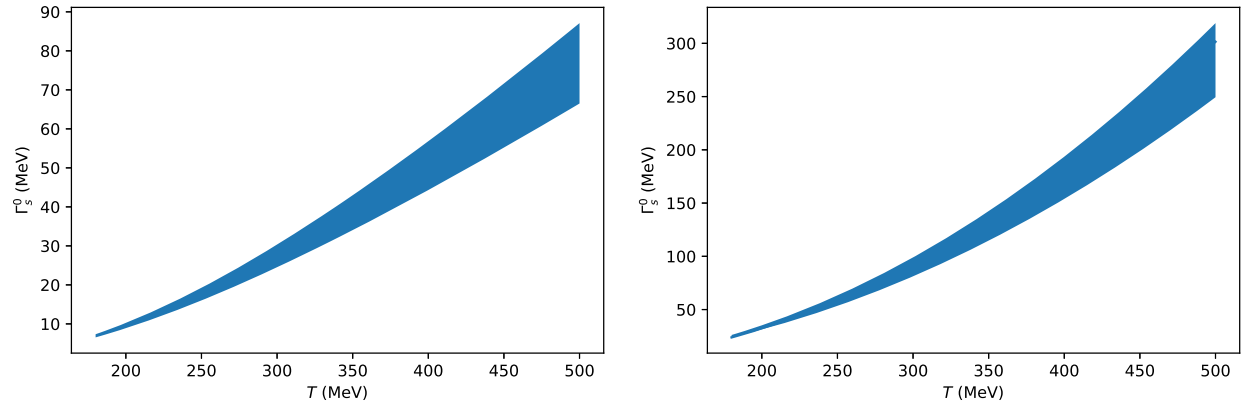

FIG. 8. The decay width Γ_s^0 of $\Upsilon(1S)$ (left) and $\Upsilon(2S)$ (right) in the lattice scenario.

of $\Upsilon(2S)$, with the difference that the effect of the gap is much less pronounced here.

We have repeated the analysis for Γ_s^0 (Fig. 8). The values that we obtained for Γ_s^0 are substantially larger than those of Γ_s, as it should, as long as we remain in the temperature region used in [42]. We observe, however, that at large temperatures Γ_s in Fig. 7 is actually larger than Γ_s^0 in Fig. 8. We view this as an artifact of extrapolating the results using Eq. (20) far beyond the region in which we performed the fit. This indicates that we have to be cautious when interpreting our results in the lattice scenario for collisions that probe high temperatures.

TABLE II. Parameters obtained by fitting the decay width in the three cases (from S1 to S3) described in the text. The parameters $\tilde{a}$ and $\tilde{b}$ correspond to the fit of the function of Eq. (20) for the case of $\Upsilon(1S)$. The parameters a and b correspond to the fit of the function of Eq. (18) for the case of $\Upsilon(2S)$.

Label	$\tilde{a}$	$\tilde{b}$(MeV)	a	b(MeV)$^{-1}$
S1	22.9	217×10	−0.285	0.00160
S2	36.9	237×10	−0.258	0.00142
S3	15.3	199×10	−0.309	0.00178

III. PHENOMENOLOGICAL IMPLICATIONS

We turn now to the main objective of this paper, which is to estimate the quantitative impact of the expansion on the previous results. To do so, we shall provide a crude estimate of the observable R_{AA}. We assume that the quarkonium state, initially in a state n, starts interacting with the plasma at some (small) finite time which we choose to be $t_0 = 0.6$ fm (value taken from [50]). The survival probability is then obtained from the rate equation [see Eq. (6)]

$$\frac{\mathrm{d}p_n}{\mathrm{d}t} = -\Gamma(T(t))p_n(t), \tag{21}$$

with the initial condition $p_n(t_0) = 1$. The survival probability of a given quarkonium state is $S = p_n(t_f)$, where t_f is the time spent by the quarkonium in the plasma. Its value depends on the scenario considered and it will be specified shortly. The above calculation assumes that the temperature evolves slowly with time so that the interaction with the plasma can be treated in an adiabatic approximation. That

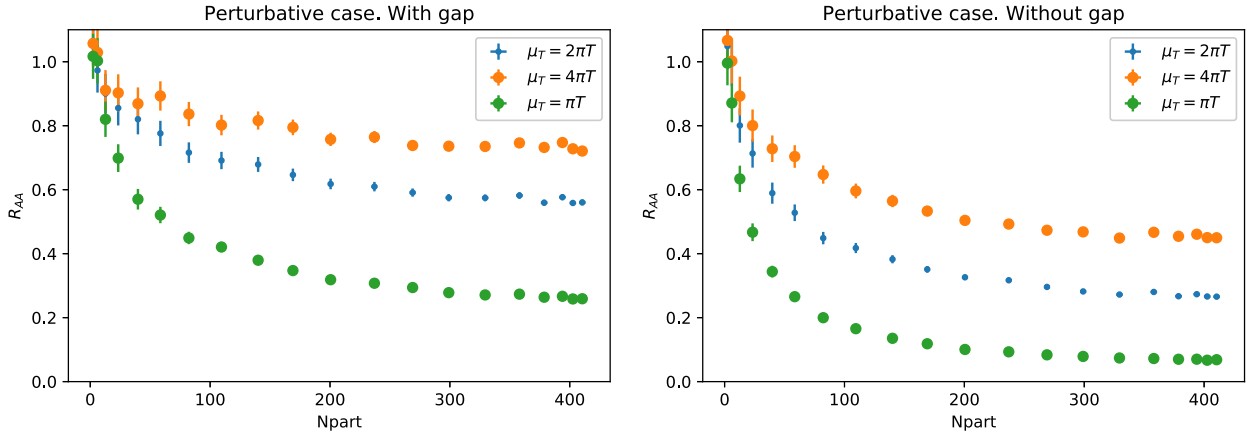

FIG. 9. R_{AA} of $\Upsilon(1S)$ obtained with the perturbative scenario against the number of participants, with (left) and without (right) the energy dependence of the decay rate. The error quoted is due to Monte Carlo integration.

is, one assumes that the quarkonium interacts with the medium as in the static case, with the medium characterized by its instantaneous temperature $T(t)$.

For simplicity, we assume that the center of mass of the quarkonium does not move in the transverse plane. Thus the survival probability depends only on the time spent in the plasma, and on the local conditions in which it evolves [51]. These depend on the impact parameter, $\boldsymbol{b}$, and on the point in the transverse plane, $\boldsymbol{s}$, (with respect to the collision axis) in which the quarkonium is produced. We set the origin of coordinates in the transverse plane to coincide with the center of one of the nucleus. The initial temperature of the medium, denoted by $T_0(\boldsymbol{b},\boldsymbol{s})$, is related to the local energy density ε by the standard relation $\varepsilon \sim T^4$. The energy density itself is taken to be proportional to the surface density of participants, which we estimate as a function of $\boldsymbol{b}$ and $\boldsymbol{s}$ using a Glauber model [52]. Thus we write

$$T_0(\boldsymbol{b},\boldsymbol{s}) = T_0(0,0)\left(\frac{T_A(\boldsymbol{s})[1-(1-\frac{\sigma T_A(\mathbf{s}-\mathbf{b})}{A})^A]}{T_A(0)[1-(1-\frac{\sigma T_A(0)}{A})^A]}\right)^{1/4}, \quad (22)$$

where T_A is the overlap function in the Glauber model, $A = 207$, and (in the type of collisions considered here) $\sigma = 70$ mb [53]. We take $T_0(0,0) = 475 \times 1.05$ TeV for $\sqrt{s} = 5.02$ TeV collisions at the LHC. This number is obtained by using the standard value of [50] and taking into account that the temperature increases by about 5% when going from 2.76 TeV collisions to 5.02 TeV collisions [54]. Regarding the time dependence of the temperature, we use Bjorken hydrodynamics, and ignore the transverse expansion,

$$T(t,\boldsymbol{b},\boldsymbol{s}) = T_0(\boldsymbol{b},\boldsymbol{s})\left(\frac{t_0}{t}\right)^{\frac{1}{3}}. \quad (23)$$

Now we have all the ingredients to compute R_{AA}. According to the optical Glauber model, R_{AA} for a given impact parameter is computed as

$$R_{AA}(\boldsymbol{b}) = \frac{\int d^2\boldsymbol{s} T_A(\boldsymbol{s}) T_A(\mathbf{s}-\mathbf{b}) S(\boldsymbol{b},\boldsymbol{s})}{\int d^2\boldsymbol{s} T_A(\boldsymbol{s}) T_A(\mathbf{s}-\mathbf{b})}, \quad (24)$$

where $S(\boldsymbol{b},\boldsymbol{s})$ is the survival probability.

A. Perturbative scenario

The survival probability can be computed analytically if we use for the decay width the approximate expression (18). One then gets

$$S_{(1S)}(\boldsymbol{b},\boldsymbol{s}) = \mathrm{e}^{-1.5aT_0(\boldsymbol{b},\boldsymbol{s})t_0((\frac{T_0(\boldsymbol{b},\boldsymbol{s})}{T_f})^2-1)-3bT_0(\boldsymbol{b},\boldsymbol{s})^2 t_0(\frac{T_0(\boldsymbol{b},\boldsymbol{s})}{T_f}-1)}. \quad (25)$$

We can use this formula to compute R_{AA}. In this case, we set $T_f = 200$ MeV, arguing that a perturbative computation is only valid for temperatures above that of the phase transition. We are aware that physics at lower temperatures might modify the survival probability. However, we ignore those effects. At the moment, our aim is not to obtain a state-of-the-art phenomenological prediction, but to highlight the importance of the energy gap between singlets and octets.

In Fig. 9 we plot the results obtained by applying this formula, taking the dependence on μ_T as a measure of our theoretical uncertainty. Although the uncertainty due to μ_T is quite significant, we can clearly see the difference between Γ_s and Γ_s^0. We see that taking into account the gap increases R_{AA} by typically the same factor of ~ 2 as in the nonexpanding case. We note that in Fig. 9, and in the rest of the figures, we have plotted our results in the full range of centralities although our model is only valid when $E \gg \Gamma_s$.

B. The lattice scenario

The computation is completely analogous to what was already explained in the perturbative scenario. The only difference is that in the case of $\Upsilon(1S)$ we used a fitting

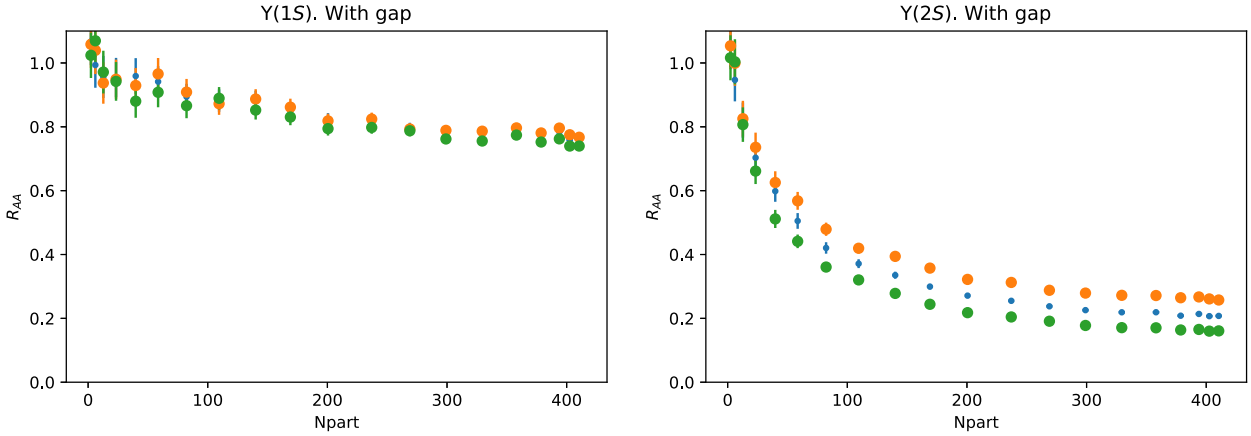

FIG. 10. Prediction for R_{AA} of $\Upsilon(1S)$ (left) and $\Upsilon(2S)$ (right) in the lattice scenario. The different symbols correspond to different parameters shown in Table II. The blue, orange, and green points correspond respectively to the S1, S2, and S3 set of parameters. Physically, the three scenarios correspond to considering the central value of m_D or the lower (larger) value of m_D compatible with the error.

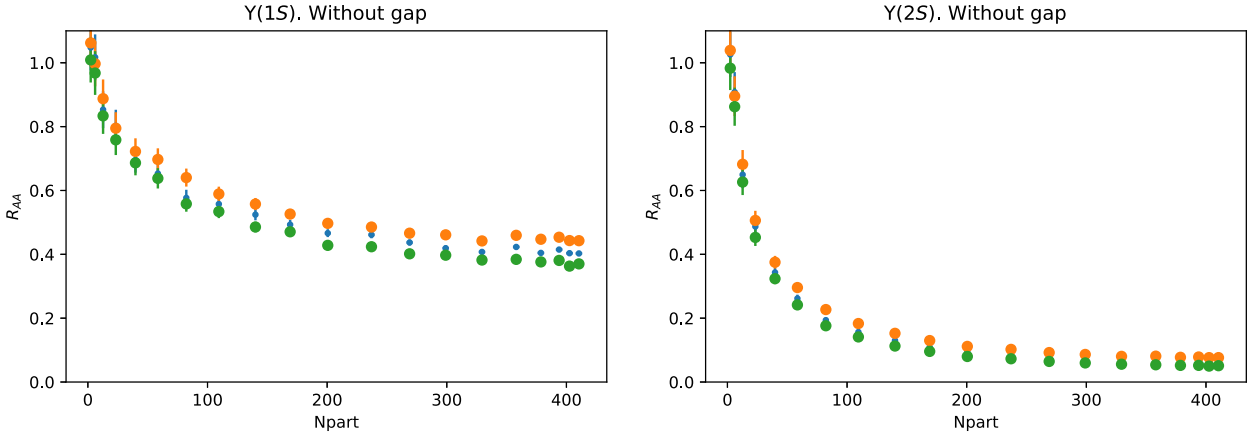

FIG. 11. Same as Fig. 10 but using Γ_s^0 instead of Γ_s.

function of the type of Eq. (20) instead of Eq. (18). In the case of a decay width which follows Eq. (20) we can also obtain an analytic solution for S,

$$S(\boldsymbol{b},\boldsymbol{s}) = e^{-\frac{3\tilde{a}T_0(\boldsymbol{b},\boldsymbol{s})^3 t_0}{\tilde{b}^2}\left(e^{-\frac{\tilde{b}}{T_0(\boldsymbol{b},\boldsymbol{s})}}\left(1+\frac{\tilde{b}}{T_0(\boldsymbol{b},\boldsymbol{s})}\right)-e^{-\frac{\tilde{b}}{T_f}}\left(1+\frac{\tilde{b}}{T_f}\right)\right)}. \quad (26)$$

In the case of $\Upsilon(2S)$, we can also apply Eq. (25). Another difference with respect to the perturbative scenario is that now we use $T_f = 180$ MeV. As we explained before, for temperatures smaller than this value, the fit obtained in [42] gives values for the energy gap between $\Upsilon(1S)$ and unbound states that are bigger than the experimental value of the difference between the mass of $\Upsilon(1S)$ and two B mesons. Therefore, we assume that at such small temperatures there are no sizeable thermal effects.

Knowing this, we obtain the R_{AA} results shown in Fig. 10. In the case of $\Upsilon(1S)$, the condition that the binding energy is much bigger than the decay width is fulfilled for a wide range of centralities. However, for $\Upsilon(2S)$ this is not the case. In fact, the validity range of our approximations for $\Upsilon(2S)$ in the lattice scenario is similar to the one of $\Upsilon(1S)$ in the perturbative case. In Fig. 11 we do the same but ignore the gap. As in the perturbative case, we see that the difference is quite substantial (again a factor of ∼2). Comparing Figs. 11 and 10 one can see that this factor can be essential to bringing the R_{AA} in agreement with its experimental value. This is approximately the case in Fig. 10, although no strong conclusion can be drawn from this remark, given the simplifications made in the present analysis. In fact, the results in Fig. 10 slightly underpredict the experimentally observed suppression, but this includes, among other things, a sizeable contribution from cold nuclear matter effects that are ignored in the present analysis.

IV. CONCLUSIONS

In this work, we have explored the phenomenological consequences of the observations made in [21], where we

highlighted the importance of taking into account the energy gap between singlet and octet states when computing the decay width of a quarkonium bound state in a medium. The role of this energy gap can be understood as an energy dependence in the imaginary potential used to determine the bound state properties. The discussion in [21] was limited to the case of a static medium. In the present study, we have extended the analysis to the case of an expanding medium, and explored the predictions of a simple model in two different scenarios, one based on perturbative formulae, and a scenario based on the lattice QCD data of [42]. Our results have corroborated our initial findings, and indicate that the role of the energy dependence of the imaginary potential is as important in the expanding case as it is in the static medium: the value of R_{AA} is significantly lower when the energy dependence is ignored. The effect is sizeable, the energy dependence reducing the expected suppression by typically a factor of 2 for bottomonium at present LHC energies.

ACKNOWLEDGMENTS

This study was triggered by discussions initiated in the EMMI Rapid Reaction Task Force Suppression and (re) generation of quarkonium in heavy-ion collisions at the LHC. M. A. E. received financial support from Xunta de Galicia (Centro singular de investigacin de Galicia accreditation 2019-2022), the European Union ERDF, the Maria de Maeztu Units of Excellence program MDM2016-0692, the Spanish Research State Agency, and from the European Research Council project ERC-2018-ADG-835105 YoctoLHC.

[1] A. M. Sirunyan *et al.* (CMS Collaboration), Measurement of nuclear modification factors of $\Upsilon(1S)$, $\Upsilon(2S)$, and $\Upsilon(3S)$ mesons in PbPb collisions at $\sqrt{s_{\mathrm{NN}}} = 5.02$ TeV, Phys. Lett. B **790**, 270 (2019).

[2] S. Acharya *et al.* (ALICE Collaboration), Υ production and nuclear modification at forward rapidity in Pb-Pb collisions at $\sqrt{s_{\mathrm{NN}}} = 5.02$ TeV, arXiv:2011.05758.

[3] M. Aaboud *et al.* (ATLAS Collaboration), Prompt and nonprompt J/ψ and $\psi(2S)$ suppression at high transverse momentum in 5.02 TeV Pb + Pb collisions with the ATLAS experiment, Eur. Phys. J. C **78**, 762 (2018).

[4] T. Matsui and H. Satz, J/ψ suppression by quark-gluon plasma formation, Phys. Lett. B **178**, 416 (1986).

[5] M. Laine, O. Philipsen, P. Romatschke, and M. Tassler, Real-time static potential in hot QCD, J. High Energy Phys. 03 (2007) 054.

[6] A. Beraudo, J. P. Blaizot, and C. Ratti, Real and imaginary-time Q anti-Q correlators in a thermal medium, Nucl. Phys. **A806**, 312 (2008).

[7] N. Brambilla, J. Ghiglieri, A. Vairo, and P. Petreczky, Static quark-antiquark pairs at finite temperature, Phys. Rev. D **78**, 014017 (2008).

[8] P. Braun-Munzinger and J. Stachel, (Non)thermal aspects of charmonium production and a new look at J/psi suppression, Phys. Lett. B **490**, 196 (2000).

[9] R. L. Thews, M. Schroedter, and J. Rafelski, Enhanced J/ψ production in deconfined quark matter, Phys. Rev. C **63**, 054905 (2001).

[10] N. Borghini and C. Gombeaud, Heavy quarkonia in a medium as a quantum dissipative system: Master equation approach, Eur. Phys. J. C **72**, 2000 (2012).

[11] Y. Akamatsu, Heavy quark master equations in the Lindblad form at high temperatures, Phys. Rev. D **91**, 056002 (2015).

[12] Y. Akamatsu, M. Asakawa, S. Kajimoto, and A. Rothkopf, Quantum dissipation of a heavy quark from a nonlinear stochastic Schrödinger equation, J. High Energy Phys. 07 (2018) 029.

[13] J.-P. Blaizot, D. De Boni, P. Faccioli, and G. Garberoglio, Heavy quark bound states in a quark–gluon plasma: Dissociation and recombination, Nucl. Phys. **A946**, 49 (2016).

[14] N. Brambilla, M. A. Escobedo, J. Soto, and A. Vairo, Quarkonium suppression in heavy-ion collisions: An open quantum system approach, Phys. Rev. D **96**, 034021 (2017).

[15] N. Brambilla, M. A. Escobedo, J. Soto, and A. Vairo, Heavy quarkonium suppression in a fireball, Phys. Rev. D **97**, 074009 (2018).

[16] S. Kajimoto, Y. Akamatsu, M. Asakawa, and A. Rothkopf, Dynamical dissociation of quarkonia by wave function decoherence, Phys. Rev. D **97**, 014003 (2018).

[17] R. Katz and P. B. Gossiaux, The Schrödinger–Langevin equation with and without thermal fluctuations, Ann. Phys. (Amsterdam) **368**, 267 (2016).

[18] X. Yao and T. Mehen, Quarkonium in-medium transport equation derived from first principles, Phys. Rev. D **99**, 096028 (2019).

[19] X. Yao and B. Müller, Quarkonium inside the quark-gluon plasma: Diffusion, dissociation, recombination, and energy loss, Phys. Rev. D **100**, 014008 (2019).

[20] J.-P. Blaizot and M. A. Escobedo, Quantum and classical dynamics of heavy quarks in a quark-gluon plasma, J. High Energy Phys. 06 (2018) 034.

[21] J.-P. Blaizot and M. A. Escobedo, Approach to equilibrium of a quarkonium in a quark-gluon plasma, Phys. Rev. D **98**, 074007 (2018).

[22] X. Yao and T. Mehen, Quarkonium semiclassical transport in quark-gluon plasma: Factorization and quantum correction, J. High Energy Phys. 02 (2021) 062.

[23] Y. Akamatsu, Quarkonium in quark-gluon plasma: Open quantum system approaches re-examined, arXiv: 2009.10559.

[24] X. Yao, Open quantum systems for quarkonia, Int. J. Mod. Phys. A **36**, 2130010 (2021).
[25] By this we mean that non diagonal elements of the density matrix play a role, not only the diagonal ones that are kept in elementary transport approaches.
[26] V. Gorini, A. Kossakowski, and E. C. G. Sudarshan, Completely positive dynamical semigroups of N level systems, J. Math. Phys. (N.Y.) **17**, 821 (1976).
[27] G. Lindblad, On the generators of quantum dynamical semigroups, Commun. Math. Phys. **48**, 119 (1976).
[28] N. Brambilla, M. A. Escobedo, M. Strickland, A. Vairo, P. Vander Griend, and J. H. Weber, Bottomonium suppression in an open quantum system using the quantum trajectories method, J. High Energy Phys. 05 (2021) 136.
[29] X. Yao and B. Müller, Approach to equilibrium of quarkonium in quark-gluon plasma, Phys. Rev. C **97**, 014908 (2018); Erratum, Phys. Rev. C **97**, 049903 (2018).
[30] This observation is also valid beyond perturbation theory [31].
[31] M. A. Escobedo, Medium evolution of a static quark-antiquark pair in the large N_c limit, Phys. Rev. D **103**, 034010 (2021).
[32] R. D. Pisarski, Scattering Amplitudes in Hot Gauge Theories, Phys. Rev. Lett. **63**, 1129 (1989).
[33] E. Braaten and R. D. Pisarski, Soft amplitudes in hot gauge theories: A general analysis, Nucl. Phys. **B337**, 569 (1990).
[34] J. Frenkel and J. C. Taylor, High temperature limit of thermal QCD, Nucl. Phys. **B334**, 199 (1990).
[35] Here we refer to the static limit as the limit $T \gg \Delta E$. Note that in other context the static limit is understood as the limit in which the heavy quark mass is infinite.
[36] D. Kharzeev and H. Satz, Quarkonium interactions in hadronic matter, Phys. Lett. B **334**, 155 (1994).
[37] D. Kharzeev, Quarkonium interactions in QCD, Proc. Int. Sch. Phys. Fermi **130**, 105 (1996).
[38] G. D. Moore and D. Teaney, How much do heavy quarks thermalize in a heavy ion collision?, Phys. Rev. C **71**, 064904 (2005).
[39] J. Casalderrey-Solana and D. Teaney, Heavy quark diffusion in strongly coupled $N = 4$ Yang-Mills, Phys. Rev. D **74**, 085012 (2006).
[40] W. Lucha and F. F. Schoberl, Solving the Schrodinger equation for bound states with Mathematica 3.0, Int. J. Mod. Phys. C **10**, 607 (1999).
[41] A. H. Hoang, 1S and MS-bar bottom quark masses from Upsilon sum rules, Phys. Rev. D **61**, 034005 (1999).
[42] D. Lafferty and A. Rothkopf, Improved Gauss law model and in-medium heavy quarkonium at finite density and velocity, Phys. Rev. D **101**, 056010 (2020).
[43] A. Islam and M. Strickland, Bottomonium suppression and elliptic flow using heavy quarkonium quantum dynamics, J. High Energy Phys. 03 (2021) 235.
[44] L. Thakur, N. Haque, and Y. Hirono, Heavy quarkonia in a bulk viscous medium, J. High Energy Phys. 06 (2020) 071.
[45] P. Srivastava, O. Chaturvedi, and L. Thakur, Heavy quarkonia in a potential model: Binding energy, decay width, and survival probability, Eur. Phys. J. C **78**, 440 (2018).
[46] L. Thakur, U. Kakade, and B. K. Patra, Dissociation of quarkonium in a complex potential, Phys. Rev. D **89**, 094020 (2014).
[47] A. Mocsy and P. Petreczky, Color Screening Melts Quarkonium, Phys. Rev. Lett. **99**, 211602 (2007).
[48] M. Hasan and B. K. Patra, Dissociation of heavy quarkonia in a weak magnetic field, Phys. Rev. D **102**, 036020 (2020).
[49] D. Kharzeev, L. D. McLerran, and H. Satz, Nonperturbative quarkonium dissociation in hadronic matter, Phys. Lett. B **356**, 349 (1995).
[50] W. M. Alberico, A. Beraudo, A. De Pace, A. Molinari, M. Monteno, M. Nardi, F. Prino, and M. Sitta, Heavy flavors in AA collisions: Production, transport and final spectra, Eur. Phys. J. C **73**, 2481 (2013).
[51] J. P. Blaizot and J.-Y. Ollitrault, The p_T dependence of J/ψ production in hadron—nucleus and nucleus-nucleus collisions, Phys. Lett. B **217**, 392 (1989).
[52] J. P. Blaizot and J.-Y. Ollitrault, On the fate of a J/ψ produced in a nucleus-nucleus collision, Phys. Rev. D **39**, 232 (1989).
[53] C. Loizides, J. Nagle, and P. Steinberg, Improved version of the PHOBOS Glauber Monte Carlo, SoftwareX **1–2**, 13 (2015).
[54] M. Alqahtani and M. Strickland, Bulk observables at 5.02 TeV using quasiparticle anisotropic hydrodynamics, arXiv:2008.07657.